# Supporting Information

Sieben et al. 10.1073/pnas.1120265109

## SI Text

**SI Materials and Methods.** ***Cell and virus propagation.*** CHO cells, Madin–Darby canine kidney (MDCK) cells, and human alveolar A549 cells were grown in DMEM (PAA) supplemented with 1% penicillin/streptomycin and 10% FCS (PAA) in Petri dishes (MatTek). For sialic acid digestion we used neuraminidase (NA) from *Clostridium perfringens* (Sigma) solved in PBS buffer. The cells were treated for 10 min at 37 °C with 1 U/mL NA. Influenza A (H3N2) virus X-31 was grown on chicken eggs and prepared as described previously (1). The HA gene was analyzed by sequencing to make sure the binding pocket is identical to the HA used for molecular dynamics (MD) simulations (2) (Fig. S2). Influenza A/WSN/33 (H1N1) was grown in MDCK cells in DMEM supplemented with 0.2% BSA (Sigma) and 4 μg/mL L-1-tosylamido-2-phenylethyl chloromethyl ketone (TPCK) trypsin (Sigma).

***Atomic force microscopy (AFM) tip chemistry.*** Commercially available AFM cantilevers (Veeco Instruments) were amine functionalized as described by using the room-temperature method for reaction with ethanolamine hydrochloride. A heterobifunctional PEG linker [aldehyde–PEG–NHS (N-hydroxysuccinimide)] was attached by incubating the tip for 2 h in 0.5 mL of chloroform containing 6.6 mg/mL aldehyde–PEG–NHS and 0.5% triethylamine, resulting in acylation of surface-linked ethanolamine by the NHS group. After rinsing with chloroform and drying, the tips were incubated in a mixture of 50 μL of approximately 0.05 mg/mL influenza A X-31 in PBS and 2 μL of 1 M $NaCNBH_3$ (freshly prepared by dissolving 32 mg of solid $NaCNBH_3$ in 500 μL of 10 mM NaOH) for 50 min. Then, 5 μL of 1 M ethanolamine hydrochloride (adjusted to pH 9.6 with 20% NaOH) was added and incubation was continued for 10 min to block unreacted aldehyde groups. The specificity of the coupling was checked by blocking the cantilever-bound PEG–aldehyde for 30 min with 50 μL of 1 M ethanolamine (pH 9.6).

***Molecular dynamics simulations.*** First, a system for equilibration simulations was built. The protein starting structure (2) was placed in a dodecahedron box with a minimal distance of 1.5 nm from protein atoms to the box boundary. Solvent consisting of water molecules and a 1-mM concentration of sodium and chloride ions was added. An energy minimization of 1,000 steps using steepest descent was employed. A 1-ns simulation with position restraints with a force constant of 1,000 kJ/mol/$nm^2$ on all heavy atoms of protein and sugar molecules was performed to equilibrate the solvent. Afterwards, 150 ns of equilibrium simulation were performed. As starting structure for the unbinding simulations, a snapshot from the equilibrium simulations after 20 ns was taken. This snapshot was aligned along its principal axes, and a triclinic box with a distance of 1.5 nm to the protein atoms was created. This box was elongated by 5 nm in pull direction to provide sufficient space for unbound sugar molecules (Fig. S5, *Lower*). The addition of solvent, energy minimization, and equilibration of solvent molecules was performed as described above. For the unbinding simulations, position restraints with a spring constant of 1,000 kJ/mol/$nm^2$ were applied to the Cα atoms of the C termini of the tail units of HA (Fig. S5, *Lower*, red circles). Three independent pulling potentials with a spring constant of 500 kJ/mol/$nm^2$ were applied to the outermost carbon atom of each sugar molecule with respect to the protein (Fig. S5 *A–C*, *Lower*, spheres and arrows). To unbind the sugar molecules from HA, the pulling potentials were moved away from the protein at constant velocity.

***Preparation and optimization of virus-coated beads.*** The virus (1 mg/mL) was labeled with 20 μM octadecylrhodamine B (R18; Invitrogen) for 30 min at room temperature. Unbound R18 was removed by centrifugation for 5 min at 50,000 × *g*. The pellet was resuspended in PBS. The virus was diluted to 20 μg/mL in PBS and viral aggregates were removed with a 200-nm pore–size sterile filter. Polystyrene (PS) beads (0.1% solids) were added and both were incubated for 30 min at room temperature. Unbound virus was removed by centrifugation. At high concentration the virus particles adsorbed to the bead surface without visible gaps (Fig. S1*A*). To increase the chance of single-virus binding events the virus suspension was diluted before addition of the PS beads. The fluorescence per bead was visualized by confocal microscopy and quantified by flow cytometry (Fig. S1*B*). Dilution of virus particles during the adsorption reduced the amount of bound virus by up to 90%. To fill the gaps between viruses, the beads were further incubated with BSA. Finally, the beads were washed in PBS and stored at 4 °C.

***Force spectroscopy data analysis.*** Force distance curves were analyzed using MatLab (MathWorks Inc.) and Igor Pro (Wavemetrics Inc.). The loading rates were determined by multiplying the pulling velocity with the effective spring constant (i.e., the mean slope at rupture). In the single-barrier model (3), the most probable rupture force, $F$, is given as a function of the loading rate, $r$:

$$F(r) = \frac{k_B T}{x_u} \ln\left(\frac{r x_u}{k_{off} k_B T}\right), \qquad \text{[S1]}$$

where $k_B$ is the Boltzmann constant, $k_{off}$ is the dissociation rate constant of the complex without force, and $x_u$ marks the thermally averaged projection of the transition state along the direction of the force. The parameters $x_u$ and $k_{off}$ were determined by fitting the most probable rupture force $F$ against the applied loading rate $r$.

***Lectin binding assay.*** MDCK, CHO, and A549 cells were washed with PBS and incubated with WGA–FITC (Wheat germ agglutinin, 40 μg/mL) or SNA–FITC (*Sambucus nigra* lectin, 10 μg/mL)/MAA–Rhodamine (*Maackia amurensin* lectin, 50 μg/mL) for 20 min at 4 °C. The cells where imaged by confocal microscopy and the lectin signals were quantified by flow cytometry (Fig. S4). For NA treatment the cells were incubated with 1 U/mL NA for 10 min at 37 °C, washed, and labeled as above. WGA–FITC was purchased from Sigma; SNA–FITC and MAA–Rhodamine were purchased from EY Labs. For flow cytometry the cells were detached form the culture dish using 2 mM EDTA in PBS.

***Fluorescence-based virus–cell binding assay.*** Influenza A/X-31 (H3N2) and A/WSN/33 (H1N1) viruses were labeled with 20 μM octadecylrhodamine B (R18) for 30 min at room temperature. Unbound dye was removed by centrifugation (50,000 × *g*, 5 min) and the virus was resuspended in PBS. Approximately $5 \cdot 10^5$ cells were incubated with 5 μg labeled virus for 20 min at 4 °C. The cells were washed and the R18 signal per cell was quantified by flow cytometry using a FACSAria II flow cytometer (Becton Dickinson).

***Sequence determination of hemagglutinin from intact viruses.*** Influenza A X-31 viruses were grown in chicken eggs and prepared as described previously (1). Genomic RNA was isolated from 1 mg virus using the Qiagen RNeasy Kit. Purified RNA was sent for sequencing.

1. Korte T, Ludwig K, Huang Q, Rachakonda PS, Herrmann A (2007) Conformational change of influenza virus hemagglutinin is sensitive to ionic concentration. *Eur Biophys J* 36:327–335.
2. Eisen MB, Sabesan S, Skehel JJ, Wiley DC (1997) Binding of the influenza A virus to cell-surface receptors: Structures of five hemagglutinin–sialyloligosaccharide complexes determined by X-ray crystallography. *Virology* 232:19–31.
3. Evans E, Ritchie K (1997) Dynamic strength of molecular adhesion bonds. *Biophys J* 72:1541–1555.

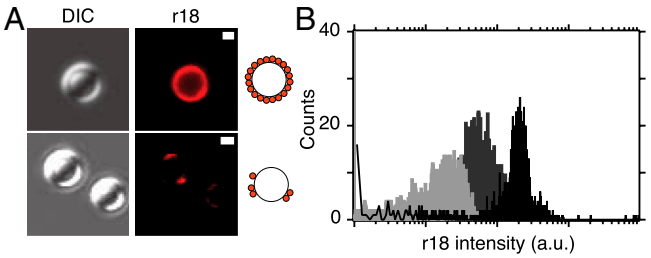


**Fig. S1.** Coating of PS beads with influenza A virus. R18-labeled influenza virions were adsorbed to polystyrene beads and the load was verified by confocal microscopy (*A*) and flow cytometry (*B*). At high virus concentration the beads were fully covered (*A*, *Upper*) and showed a high mean R18 intensity (*B*, black histogram). Dilution of the virus led to a reduction of virus particles on the bead surface (*A*, *Lower*). The mean R18 intensity per bead was reduced by 50% and 80%, respectively (*B*, gray and light gray histograms). Scale bar, 0.5 μm.

```
this study      MKTIIALSYIFCLALGQDLPGNDNSTATLCLGHHAVPNGTLVKTITDDQIEVTNATELVQ 60
Eisen et al.    MKTIIALSYIFCLALGQDLPGNDNSTATLCLGHHAVPNGTLVKTITDDQIEVTNATELVQ 60
                ************************************************************

this study      SSSTGKICNNPHRILDGIDCTLIDALLGDPHCDVFQNETWDLFVERSKAFSNCYPYDVPD 120
Eisen et al.    SSSTGKICNNPHRILDGIDCTLIDALLGDPHCDVFQNETWDLFVERSKAFSNCYPYDVPD 120
                ************************************************************

this study      YASLRSLVASSGTLEFITEGFTWTGVTQNGGSNACKRGPGSGFFSRLNWLTKSGSTYPVL 180
Eisen et al.    YASLRSLVASSGTLEFITEGFTWTGVTQNGGSNACKRGPGSGFFSRLNWLTKSGSTYPVL 180
                ************************************************************

this study      NVTMPNNDNFDKLYIWGIHHPSTNQEQTSLYVQASGRVTVSTRRSQQTIIPNIGSRPWVR 240
Eisen et al.    NVTMPNNDNFDKLYIWGIHHPSTNQEQTSLYVQASGRVTVSTRRSQQTIIPNIGSRPWVR 240
                ************************************************************

this study      GLSSRISIYWTIVKPGDVLVINSNGNLIAPRGYFKMRTGKSSIMRSDAPIDTCISECITP 300
Eisen et al.    GLSSRISIYWTIVKPGDVLVINSNGNLIAPRGYFKMRTGKSSIMRSDAPIDTCISECITP 300
                ************************************************************

this study      NGSIPNDKPFQNVNKITYGACPKYVKQNTLKLATGMRNVPEKQTRGLFGAIAGFIENGWE 360
Eisen et al.    NGSIPNDKPFQNVNKITYGACPKYVKQNTLKLATGMRNVPEKQTRGLFGAIAGFIENGWE 360
                ************************************************************

this study      GMIDGWYGFRHQNSEGTGQAADLKSTQAAIDQINGKLNRVIEKTNEKFHQIEKEFSEVEG 420
Eisen et al.    GMIDGWYGFRHQNSEGTGQAADLKSTQAAIDQINGKLNRVIEKTNEKFHQIEKEFSEVEG 420
                ************************************************************

this study      RIQDLEKYVEDTKIDLWSYNAELLVALENQHTIDLTDSEMNKLFEKTRRQLRENAEDMGN 480
Eisen et al.    RIQDLEKYVEDTKIDLWSYNAELLVALENQHTIDLTDSEMNKLFEKTRRQLRENAEEMGN 480
                ************************************************************:***

this study      GCFKIYHKCDNTCIESIRNGTYDHDVYRDEALNNRFQIKGVELKSGYKDWILWISFAISC 540
Eisen et al.    GCFKIYHKCDNACIESIRNGTYDHDVYRDEALNNRFQIKGVELKSGYKDWILWISFAISC 540
                ***********:************************************************

this study      FLLCVVLLGFIMWACQRGNIRCNICI 566
Eisen et al.    FLLCVVLLGFIMWACQRGNIRCNICI 566
                *************************
```

**Fig. S2.** HA sequence alignment. Genomic RNA was isolated from influenza A X-31 viruses (1 mg) using the Qiagen RNeasy Kit. The obtained sequence was compared with the X-31 amino acid sequence from Eisen et al. (1). The HA1 subunit containing the receptor binding site is marked in red.

1 Eisen MB, Sabesan S, Skehel JJ, Wiley DC (1997) Binding of the influenza A virus to cell-surface receptors: Structures of five hemagglutinin–sialyloligosaccharide complexes determined by X-ray crystallography. *Virology* 232:19–31.

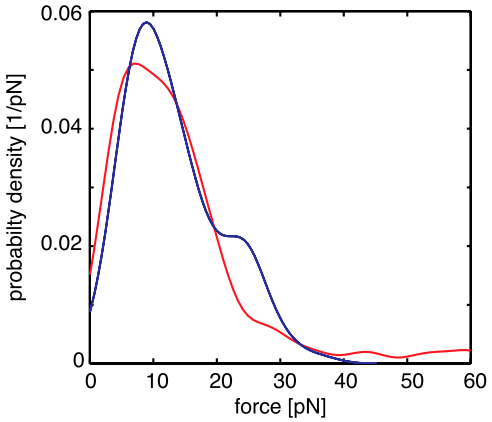


**Fig. S3.** SVFS measurements using optical tweezers. Distribution of rupture forces from MDCK cells shows a second maximum at approximately 23 pN (blue curve), which was not well-pronounced in the case of CHO cells (red curve). The second peak corresponds to the simultaneous rupture of two bonds.

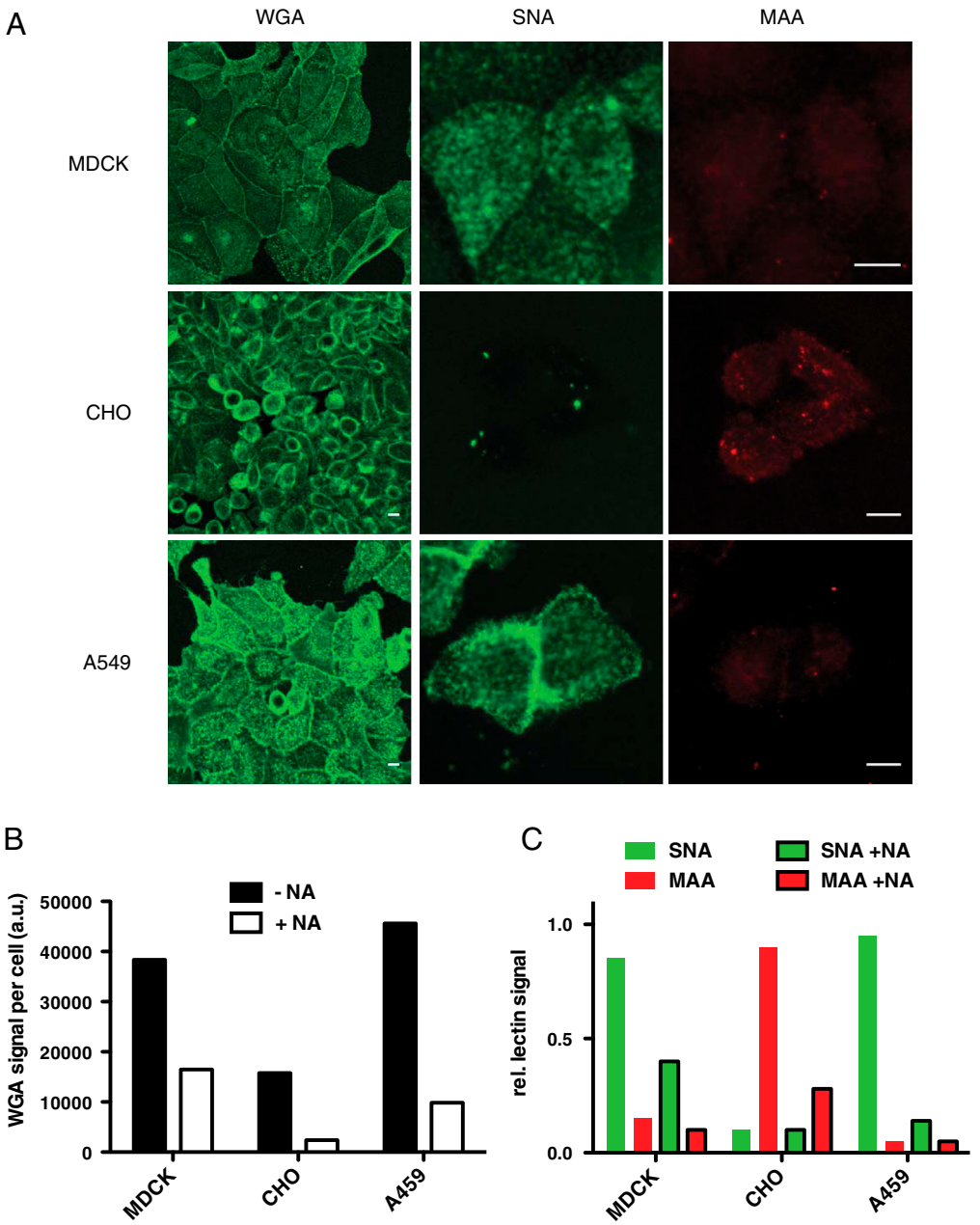


**Fig. S4.** Surface sialic acid characterization by confocal microscopy and flow cytometry. MDCK, CHO, and A549 cells were washed with PBS and incubated with WGA–FITC (40 μg/mL) or SNA–FITC (10 μg/mL)/MAA–Rhodamine (50 μg/mL) for 20 min at 4 °C. The cells were imaged by confocal microscopy (*A*) and the lectin signals were quantified by flow cytometry (*B* and *C*). For NA treatment the cells where incubated with 1 U/mL NA for 10 min at 37 °C, washed, and labeled as above. MDCK and A549 cells predominantly present 2,6–linked SA, whereas CHO cells mostly present 2,3–linked SA. Neuraminidase treatment reduced both fractions. Because of its limited specificity, MAA can hardly be used to express the degree of 2,3–linked SA on the cell surface. However, for a better presentation we calculated relative abundances of 2,3–and 2,6–linked SA (*B*).

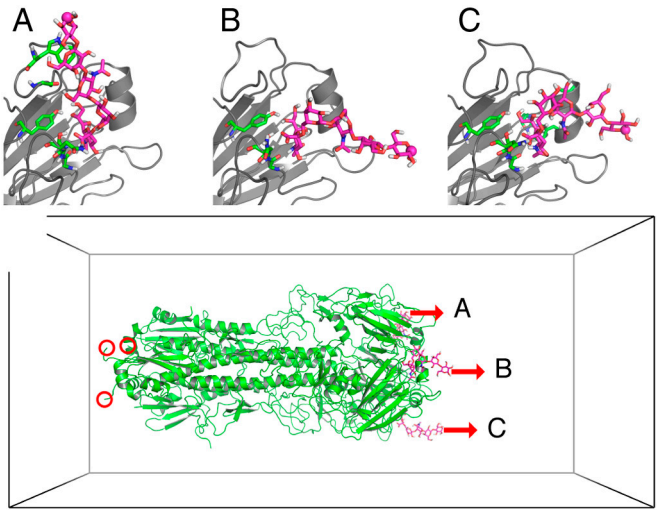


**Fig. S5.** Receptor conformations and simulation setup. (*Upper*) Receptor conformations A, B, and C. The receptors (magenta) and interacting residues of HA (green) are shown as sticks. HA is shown in white cartoon representation. All pulling potentials are moved to the right. (*Lower*) HA (green, cartoon) and all three bound receptors (magenta, sticks) are shown within the simulation box (black lines). Position restraints on HA are shown as red circles. Three individual pulling potentials were applied to the receptors (red arrows).

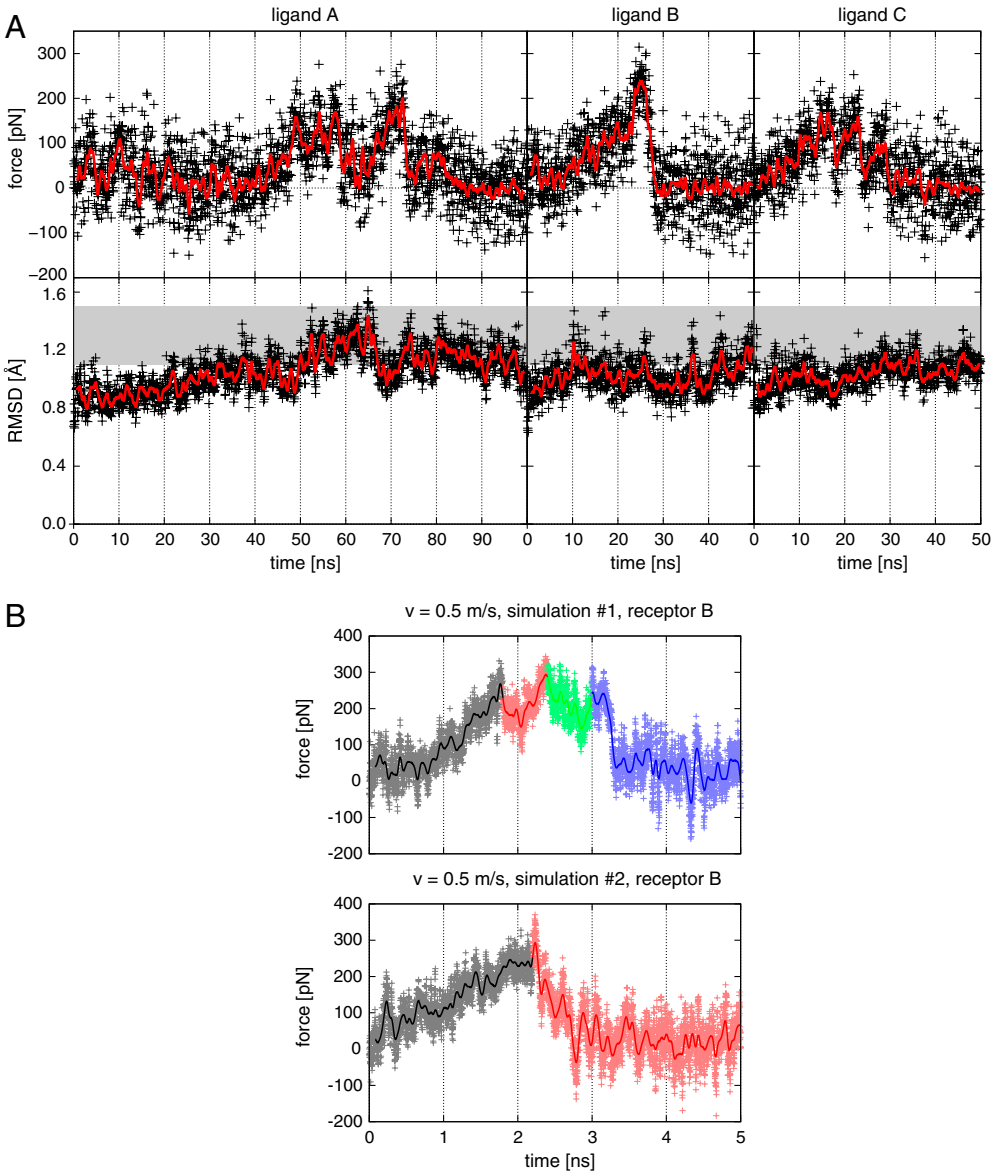


**Fig. S6.** A rmsd plot of the HA head domain during unbinding of all three receptors (*A*). Two unbinding simulations of receptor B at the same retraction speed illustrate the diversity of unbinding pathways (*B*).

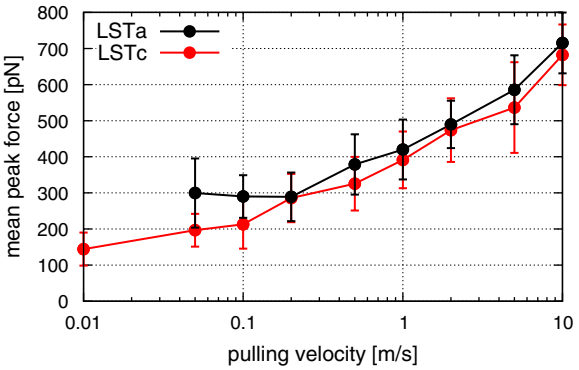


**Fig. S7.** Comparison of mean peak forces obtained from MD simulations with lactoseries tetrasaccharide a and c (LSTa and LSTc). The MD datapoints represent the mean rupture force of all unbinding events at the indicated pulling velocity.

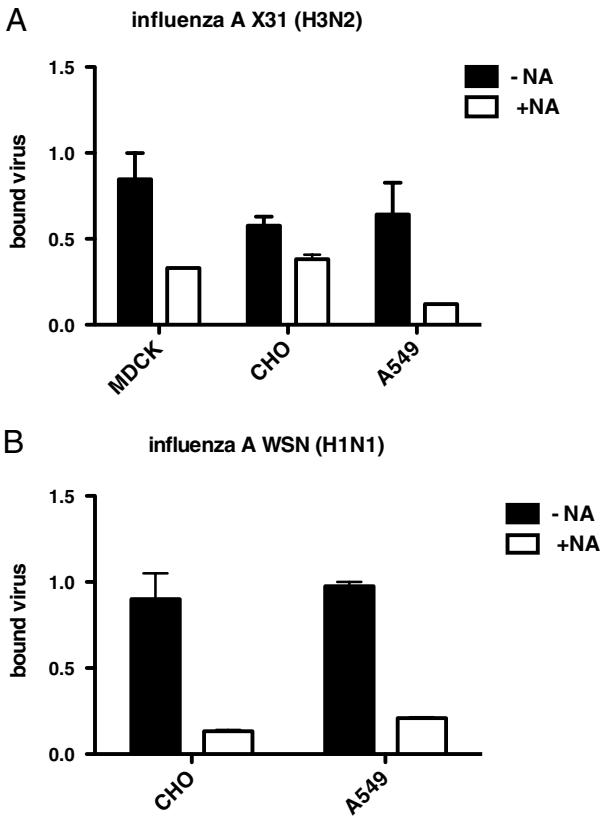


**Fig. S8.** Fluorescence-based virus binding assay. Influenza A X-31 (H3N2) and A/WSN/33 (H1N1) viruses were labeled with R18 (20 μM) for 30 min at room temperature. Unbound dye was removed by centrifugation (50,000 × *g*, 5 min) and the virus was resuspended in PBS. Approximately $5 \cdot 10^5$ cells were incubated with 5 μg labeled virus for 20 min at 4 °C. The cells were washed and the R18 signal per cell was quantified by flow cytometry. The plots show mean and SEM of three independent comparative experiments using H3N2 (*A*) and H1N1 (*B*) viruses. Each signal was normalized to the maximum fluorescence within each experiment.

**Movie S1.** One optical tweezers experiment. A virus-coated bead was moved toward a CHO cell until touching the surface and then retracted without delay. The rupture event is clearly visible.

Movie S1 (AVI)

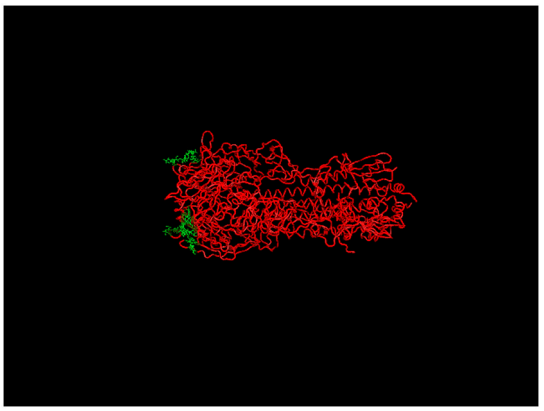

**Movie S2.** One force-probe molecular dynamics simulation between one HA trimer (red) and all three receptors (green). Pulling speed: 0.1 m/s.

Movie S2 (MOV)

**Table S1. Hydrogen bonds between HA residues and different receptor conformations (as introduced in Fig. S5)**

| Residue | Receptor A | Receptor B | Receptor C |
|---|---|---|---|
| Tyr98 | X | X | X |
| Gly135 | X | X | X |
| Ser136 | X | X | X |
| Asn137 | X | X | X |
| Thr187 | | | X |
| Glu190 | | | X |
| Ser193 | | | X |
| Trp222 | X | | |
| Gly225 | X | | |